Poly(N-isopropylacrylamide) / poly(l-lactic acid-co-ε-caprolactone) fibers loaded with ciprofloxacin as wound dressing materials

Heyu Li[1], Gareth R. Williams[2], Junzi Wu[1], Haijun Wang[1], Xiaozhu Sun[1], Li-Min Zhu[1*]

1. College of Chemistry, Chemical Engineering and Biotechnology, Donghua University，Shanghai, 201620, China

2. UCL School of Pharmacy, 29-39 Brunswick Square, London, WC1N 1AX, UK

*Corresponding author:

E-mail: lzhu@dhu.edu.cn Tel：+862167792655

Abstract:

In this work, we aimed to develop new materials to reduce the secondary injuries which can be imparted when replacing wound dressings. Electrospun fibers based on the thermoresponsive polymer poly(N-isopropylacrylamide) (PNIPAAm), poly(l-lactic acid-co-ε-caprolactone) (PLCL), and the antibiotic ciprofloxacin (CIF) were prepared. The water contact angle of fibers made from a blend of PNIPAAm and PLCL changed dramatically when the temperature was increased above 32 °C. Sustained release of CIF from the formulations was observed over more than 200 h. Moreover, L929 fibroblasts could proliferate on the fibers, indicating their biocompatibility. The CIF-loaded fibers were found to have potent antibacterial activity against *E. coli* and *S. Aureus*. *In vivo* tests on rats indicated that CIF-loaded thermosensitive fibers have enhanced healing performance compared to CIF loaded PLCL fibers or a commercial gauze. Electrospun PNIPAAm/PLCL fibers loaded with CIF thus have great promise in the development of new wound dressing materials.

Keywords: wound dressing, electrospinning, thermosensitive, PNIPAAm, antibacterial.

1. Introduction:

Wound healing is a complicated biological process involving numerous physiological factors. To accelerate the healing process, wound dressings have been used since ancient times [1]. Modern dressings must both provide basic protection for the wound site and also accelerate the healing process [2, 3]. Various materials have been reported in the literature in attempts to achieve the latter, including foams, films, hydrocolloids, hydrogels, and hydrofibers (*inter alia*) [4-8]. Electrospun fibers have attracted much attention in this regard, and have a number of potential advantages as wound dressing materials.

Electrospinning is a simple and effective method for producing fibers with diameters ranging from tens of nanometers to micrometers. The materials fabricated by this route not only have high porosity and surface area-to-volume ratios (with the possibilities of tuning both), but also resemble the morphological structure of the extra-cellular matrix (ECM) and generally have good biocompatibility [9-11]. As a result of these characteristics, they have hemostatic properties, and are absorbable and semi-permeable, giving great promise as wound dressing materials [12]. Furthermore, various functional ingredients can easily be incorporated into fibers *via* electrospinning [1]. This could yield multi-functional wound healing materials.

To date, a number of polymers have been used to fabricate electrospun wound dressings, including gelatin, collagen, chitosan, poly(vinyl alcohol), poly(ε-caprolactone) (PCL), and poly(L-lactic acid) [3, 13-16]. Of particular interest is poly(l-lactic acid-co-ε-caprolactone) (PLCL), a copolymer of L-lactic acid and ε-caprolactone which has outstanding mechanical properties, biocompatibility and degradability [17]. The use of electrospun PLCL scaffolds has been widely investigated in tissue regeneration [18, 19]), but has attracted much less attention in the context of wound dressing materials.

Beyond these simple systems, more complex stimuli-responsive polymers have been shown to have great promise in biomaterials, drug delivery systems and sensors [20-25]. They exhibit a change in configuration, dimensions, or physicochemical properties after exposure to an external stimulus, such as changes in temperature, pH,

electromagnetic field, or light [26-28]. Poly(N-isopropylacrylamide) (PNIPAAm) is a typical temperature-sensitive polymer. In aqueous solution it undergoes a sharp phase transition from linear to globular at a lower critical solution temperature (LCST) of 32 ^{o}C [29-31]. When the temperature is raised through the LCST, PNIPAAm changes from being hydrophilic to hydrophobic [32-34]. It has been intensively studied for potential applications in biomedicine [35-38], and has also been electrospun successfully [33, 39, 40]. Moreover, it has been found that thermosensitive materials like PNIPAAm can effectively control cell adhesion and detachment through variation in the temperature [41]. The strength of interactions between the polymer and cells is generally increased above the LCST, and thus if a polymer has an LCST a little below the human body temperature a low-temperature treatment can be applied to reduce attractions between the polymer and cells [42]. This could in turn reduce secondary injuries caused when a dressing is removed from a wound.

Several researchers have reported thermosensitive wound dressings generated from PNIPAAm [43-45]. For example, systems based on PNIPAAm, polyurethane and chitosan have been proven to exhibit good biocompatibility, antibacterial ability and water vapor transmission [46]. In other work, Yang *et al.* found that polymer membranes synthesized from PNIPAAm, methyl methacrylate, and 2-hydroxyethyl methacrylate have low cytotoxicity, promising thermosensitivity and good cell detachment properties [43], with 90% of L929 cells being detached at 15 ^{o}C. However, most of the reported thermosensitive dressings based on PNIPAAm were not fabricated by electrospinning, and we hypothesized that preparing similar systems in the form of electrospun fibers would result in a number of advantageous properties.

The work described in this paper forms part of a programme of research aiming to prepare wound dressings from electrospun fibers. We focus on blend materials containing both a thermosensitive polymer and a second material to provide the required mechanical properties. Previously, we have explored electrospun fibers based on poly(di(ethylene glycol) methyl ether methacrylate) and PLCL, and found these to be promising in reducing secondary injuries [47]. However, there remains the need to systematically explore a wide range of polymers in order to identify the optimum

system for use in the clinic, and this work builds on our previous results to investigate an alternative thermosensitive polymer. Here, we thus blended PNIPAAm and PLCL to fabricate composite fibers *via* electrospinning. Ciprofloxacin (CIF), a fluoroquinolone antibiotic, was also incorporated to provide antibacterial properties. *In vitro* and *in vivo* investigations of the CIF-loaded PNIPAAm/PLCL wound dressing materials were undertaken. This is the first time PNIPAAm/PLCL fibers have been electrospun and explored for their potential in wound dressings.

2. Experimental details

2.1 Materials

N-isopropylacrylamide (NIPAAm) was purchased from Japan TCI (Japan). Ciprofloxacin (CIF, purity ≥ 98%), phosphate-buffered saline (PBS), sodium azide, penicillin, trypsin and thiazolyl blue (MTT) were procured from Sigma-Aldrich Ltd. (USA). Azobisisobutyronitrile (AIBN), anhydrous ethanol, acetone, formaldehyde and n-hexane were obtained from the Sinopharm Chemical Reagent Co., Ltd (China). Poly(l-lactic acid-co-ε-caprolactone) (PLCL, 50:50; Mw = 34.5×10^4g/mol) was provided by Nara Medical University (Japan). 1,1,1,3,3,3-hexafluoro-2-propanol (HFIP, 99.5%) came from the Aladdin Industrial Corporation (China). L929 cells were provided by the Institute of Biochemistry and Cell Biology (Chinese Academy of Sciences, China). Dimethyl sulfoxide (DMSO) and DMEM culture medium were sourced from Jinuo Biological Medicine Technology Ltd. (China). All other chemicals used were analytical grade, and water was doubly distilled before use.

2.2 Polymerization of NIPAAm

PNIPAAm was prepared by free-radical polymerization in accordance with previous work [48]. NIPAAm (5.0 g) and AIBN (25.0 mg) were dissolved in anhydrous ethanol (10 mL) and heated at 70 ºC under a positive pressure of N_2. After 7 h, the resultant polymer was precipitated in n-hexane. This crude product was re-precipitated from 50 mL of acetone into 200 mL of n-hexane three times, and the purified material dried for 3 days in a vacuum oven (DZF-6050, Shanghai Laboratory Instrument Work Co. Ltd.,

China). Successful polymerization was verified by ^{1}H nuclear magnetic resonance (AV-400 instrument, Bruker, Germany) and IR spectroscopy (Nicolet-Nexus 670 FTIR spectrometer, Nicolet Instrument Corporation, USA). Molecular weights (Mw and Mn) and molecular weight distributions were determined by gel permeation chromatography (GPC) measurements on a Waters LS measurement system (Waters, USA) with tetrahydrofuran (THF) as the solvent. The flow rate was 1.0 mL/min, and the column temperature was 35 ºC. The molecular weight distribution was calibrated with standard polystyrene samples.

2.3 Preparation of electrospinning solutions

PNIPAAm and PLCL were co-dissolved in HFIP under magnetic stirring for 15 h at room temperature to obtain clear and homogenous solutions. The component ratios of PNIPAAm to PLCL were 1:1 or 1:2 (w/w), and the total concentration of polymer was 10 % (w/v). Solutions of PLCL alone (10 % w/v in HFIP) were also prepared as controls. The antibiotic CIF was added into the solutions at a drug to polymer ratio of 1:10 (w/w) [49]. Full details of the solutions prepared are listed in Table 1.

Table 1. Details of the electrospinning solutions prepared. The total polymer concentration was 10 % w/v in all cases.

Sample	Solution contents	PNIPAAm to PLCL ratio (w/w)	Drug concentration (% w/v)
S1	PNIPAAm/ PLCL	1:1	---
S2	PNIPAAm/ PLCL	1:2	---
S3	PLCL	---	---
S4	PNIPAAm/ PLCL /CIF	1:1	1.0
S5	PNIPAAm/ PLCL /CIF	1:2	1.0
S6	PLCL /CIF	---	1.0

2.4 Electrospinning

Each of the electrospinning solutions was placed into a 5 mL plastic syringe fitted with a stainless steel needle (internal diameter 0.5 mm), and the syringe mounted on a syringe pump (KDS100, Cole-Parmer, USA). The solution was expelled from the syringe at a rate of 1.0 mL/h and a high voltage power supply (ZGF-2000, Shanghai Sute Electrical Co. Ltd., China) used to apply a voltage of 14 kV between the needle and a grounded collector (a flat piece of aluminum foil of 12 x 12 cm in size). The distance between the needle tip and the grounded collector was fixed at 10 cm. The relative humidity was *ca.* 40 %, and the temperature 25 ºC. After electrospinning for 5 h, the products were stored in a vacuum oven at room temperature for 24 h to remove residual solvent.

2.5 Morphological observations

The morphology of the fibers was observed by scanning electron microscopy (SEM; JSM-5600 LV microscope, JEOL, Tokyo, Japan). Samples were first gold sputter-coated for 60s under argon to make them electrically conductive. They were then imaged using SEM at a voltage of 10 kV. The average fiber diameter for each sample was calculated by measuring approximately 100 fibers in SEM images, using the ImageJ software (National Institutes of Health, USA) [50].

2.6 Further characterization

Characterization was undertaken following the best-practice reported in the literature [1, 3, 10, 17, 18, 50]. X-ray diffraction (XRD) was performed on a D/Max-BR diffractometer (Rigaku, Japan). The instrument is supplied with Cu Kα radiation (1.5418 Å; 40 kV and 30 mA), and patterns were collected over the 2θ range 5-60º.

Fourier transform infrared (FTIR) spectra were obtained using a Nicolet-Nexus 670 FTIR spectrometer (Nicolet Instrument Corporation, USA) over the range 500-4000 cm^{-1}, at a resolution of 2 cm^{-1}.

The water contact angle (CA) was determined on a contact angle analyzer (DSA 30, Krüss GmbH, Germany) in air. A water droplet (*ca.* 5 µL) was placed onto the surface of the fibers and the CA recorded. The measurement temperature was varied

from 20 ºC to 45 ºC using a heating platform (XMTD-204, JTHF Company, China). Five measurements were recorded for each sample, and the results are reported as mean ± S.D.

2.7 *In vitro* drug release

Drug release experiments were conducted at 37 ºC and 110 rpm in a thermostatic shaking incubator (Jintan Instrument Co. Ltd., China). 0.1 g of each of the CIF-loaded fiber samples was immersed in 30 mL of phosphate buffer solution (PBS, pH 7.4). At predetermined time points, 1 mL of the test medium was withdrawn and an equal amount of fresh preheated PBS added to maintain the total solution volume [47, 48]. The concentration of CIF was measured using a UV-vis spectrometer (UV-1800, SHJH Company, China) at a wavelength of 269 nm. All the release studies were performed in triplicate, and the results are given as mean ± S.D.

2.8 Antibacterial activity

In this assessment, 10^5 colony forming units (CFUs) of *E. coli* (Gram-negative; ATCC 25922) and *S. aureus* (Gram-positive; ATCC 27853) were selected as representative microorganisms, and cultured in Lauria Broth (LB). First, the minimum inhibitory concentrations (MIC) of CIF against the two microorganisms were quantified using the broth method, following protocols detailed in the literature [51]. Bacteria were cultured in the appropriate medium supplemented with CIF at a concentration of 200, 100, 50, 25, 12.5, 6.25, 3.125, 1.562, 0.78 or 0 μg/mL. After culture for 24 hours, the MIC of CIF could be determined via observation of the bacterial growth.

Antibacterial activities of the fibers were studied using the disc diffusion method of the US Clinical and Laboratory Standards Institute (CLSI) [49]. The fiber samples were cut into circular discs 2 cm in diameter and sterilized by 75 % alcohol steam for 24 h. 100 μL of the bacterial suspension being studied was added to an agar plate in a Petri dish (of diameter 9.8 cm), and then the fiber discs were placed on the surface of the agar plate. All the dishes were incubated at 37 ºC for 12 h, after which the inhibition zones were then measured. Zones are reported as the diameter of the inhibition circle

observed. Six replicate experiments were performed, and the results are reported as mean ± S.D.

2.9 MTT assays

Fibers were first electrospun directly onto cover slips following protocols in the literature [17]. 20 cover slips were placed onto the collector plate and 4 mL of spinning solution was dispensed onto them. The fiber-covered slips were placed into the wells of 24-well plates, with untreated cover slips used as a negative control. Prior to cell culture experiments, the plates were sterilized with alcohol steam for 24 h. Complete DMEM medium was prepared by supplementing DMEM with 10 % v/v fetal bovine serum and 1% (v/v) of a pre-made penicillin (0.08 mg/ml) / streptomycin (0.1 mg/ml) solution.

400 μL of dissociated L929 fibroblasts (5.0×10^3 cells/mL) in complete DMEM was added to each well, and the plates placed in an incubator (37 ºC, 5 % CO_2). During the incubation period, the culture medium was replaced on a daily basis. At predetermined time points (after 1, 3, or 5 days of culture), the medium in each well was replaced by 360 μL of fresh DMEM and 40 μL of an MTT solution (5 mg/mL thiazolyl blue in PBS). After incubation for 5 hours, the solution in each well was replaced with 400 μL DMSO and the plates shaken for 30 min. The solution in each well was transferred to a 96-well plate and the absorbance measured at a wavelength of 570 nm, using a microplate reader (Multiskan FC, Thermo Scientific Instrument Co. Ltd., China). Three independent MTT assays were carried out, with 5 replicates per assay.

2.10 *In vivo* experiments

Animal experiments were performed under certificate SYZK 2014-0022 issued by the Shanghai Science and Technology Committee, in full accordance with their rules and regulations. Male SD (Sprague Dawley) rats from SLAC Laboratory Animals Inc. (China) weighing from 230-260 g were used as animal models. The animals were anesthetized with an intraperitoneal injection of pentobarbitone sodium (50 mg/kg) and

then an open excision type wound of *ca.* 3 cm × 3 cm (900 mm^2) was created to the depth of loose subcutaneous tissue on their upper backs. S4, S5 or S6 fiber mats (3 cm × 3 cm (900 mm^2)) which had been pre-sterilized by alcohol steam for 24 h were used to cover the skin wounds. A pure cotton commercial gauze was placed on top of the mats, and the gauze edge sutured to the skin around the wound area. This is in accordance with a previously reported protocol [52]. Commercial gauzes (Shanghai Yinjing Meidical Supplies Company Ltd., China) soaked with a 0.9 % w/v CIF solution were used as a control group. There were seven rats in each group.

2.11 Macroscopic observation of wound healing

After recovery from anaesthesia, the rats were housed individually in disinfected cages at a temperature of 25 ± 2 ºC. The dressings in all the groups were replaced every three days. Before replacement, the fibers and gauzes on the wounds were treated with sterile saline at 25 ºC. The appearance of the wound was photographed at selected times post-operation and the area of unhealed wound measured from the images using the Photoshop software (Adobe, USA). The relative wound area was determined as follows:

Relative wound area = $S_t/S_0 \times 100\%$

where S_t and S_0 are the wound areas on the specified day and operation day, respectively.

2.12 Histological and immunohistochemical examinations

21 days after operation, three rats from each group were sacrificed using a large dose of anesthetic. The wound sections were excised, collected and cut into small sections (*ca.* 4 µm). The sections were fixed with 10 % v/v formaldehyde in water, rinsed in water, and placed in a transparent block of melted paraffin. Care was taken to ensure that the samples were completely immersed in the block, after which the sections were fixed on a slicer for hematoxylin-eosin (HE) staining. For the latter, the sections were washed with distilled water, stained with hematoxylin, rinsed under running tap water, and differentiated with 0.3% acid alcohol. They were then again rinsed under running tap water, before being stained with eosin for 2 min, dried, cleaned and mounted. HE-stained sections were observed with the aid of a light microscope (Nikon Eclipse E400,

Japan).

2.13 Statistical analysis

Statistics analysis was performed using Origin v8.5 (Origin Lab Inc., USA). All values were determined at least in triplicate and are expressed as mean ± standard deviation (SD). Statistical differences were determined by one-way ANOVA, with differences at $p < 0.05$ considered significant.

3. Results and discussion

3.1 Synthesis of PNIPAAm

The successful synthesis of PNIPAAm was verified by ^{1}H NMR (Fig. S1). The NMR spectrum of the polymer shows no signals attributable to methylene protons (see Fig. S1(a)), whereas in that of the monomer (NIPAAm, Fig. S1(b)) vinyl peaks at *ca.* 5.5 and 6.2 ppm can clearly be seen. Instead, PNIPAAm shows peaks at around 1.4 and 2.0 ppm, typical of saturated systems and agreeing with a previous study [53], indicating the successful formation of the polymer. Similar conclusions can be drawn from FTIR spectra (Fig. S2). NIPAAm shows a sharp band at 1621 cm^{-1} (C=C stretching), which has disappeared in the spectrum of PNIPAAm. The molecular weights (Mw and Mn) and molecular weight distribution (PDI) determined by GPC were 11479 Da, 10380 Da, and 1.12, respectively.

3.2 Fiber morphology

SEM images and the calculated diameter distributions for all the electrospun materials are shown in Fig. 1. It is immediately obvious from the images that fiber formation was successful. Considering the drug-free fibers, the pure PLCL S3 fibers have the largest diameters (915 ± 116 nm). The diameters of S1 (PNIPAAm : PLCL 1:1; 898 ± 155 nm) are a little smaller, but much larger than S2 (PNIPAAm : PLCL 1:2; 699 ± 110 nm). Hence, there is no clear relationship between the content of PNIPAAm and fiber diameter. While the S1 – S3 fibers have generally smooth and cylindrical morphologies,

the CIF-loaded fibers are less uniform. Some beads can be seen on the surface of the latter, which could result from an increase in viscosity with the addition of CIF. It has been reported that increased solution viscosity can improve electrospinnability and aid the formation of smooth fibers. However, higher viscosities can also lead to the formation of beaded fibers [54, 55]. The diameters of the fibers loaded with CIF (S4-S6) are rather narrow, being smaller than the pure polymer materials in all cases. In the most extreme example, the average diameter of S6 (PLCL/CIF) is 620 ± 127 nm as compared to 915 ± 116 nm for the analogous drug-free system S3. This could be caused by an increase in conductivity following the addition of CIF, which is known to facilitate elongation of the polymer jet and to generate narrower fibers [56].

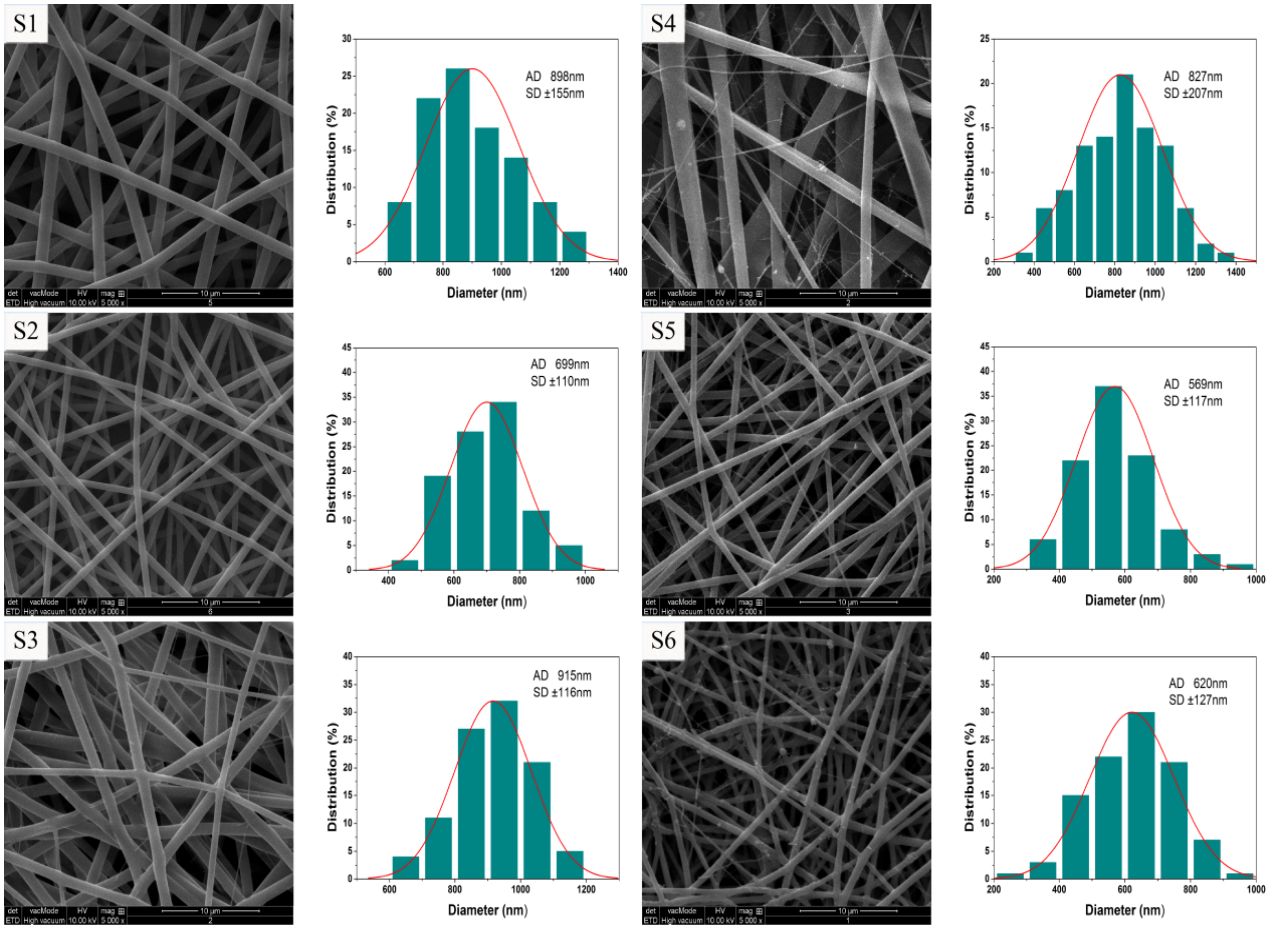

Fig. 1 SEM images and diameter distributions of the fibers produced.

3.3 X-ray diffraction

XRD patterns of the CIF-loaded fibers (S4, S5 and S6) can be seen in Fig. 2(a), along with that of pure CIF. The latter exists in a crystalline state, displaying a number of characteristic reflections between 5° and 50° 2θ. The fibers loaded with CIF display only two broad diffuse peaks centered at around 17° and 23°, and the characteristic reflections of CIF cannot be seen. Therefore, CIF is dispersed in the fibers in an amorphous state, as is commonly seen for electrospun materials. These results are in full agreement with numerous studies in the literature [47, 50, 57]. As has been widely reported, the very rapid solvent evaporation which occurs during electrospinning does not allow sufficient time for the molecular organization required for the formation of a crystal lattice from a solution. As a result, the random arrangement of molecules in the electrospinning solution is propagated into the solid state, generating amorphous materials [58, 59]

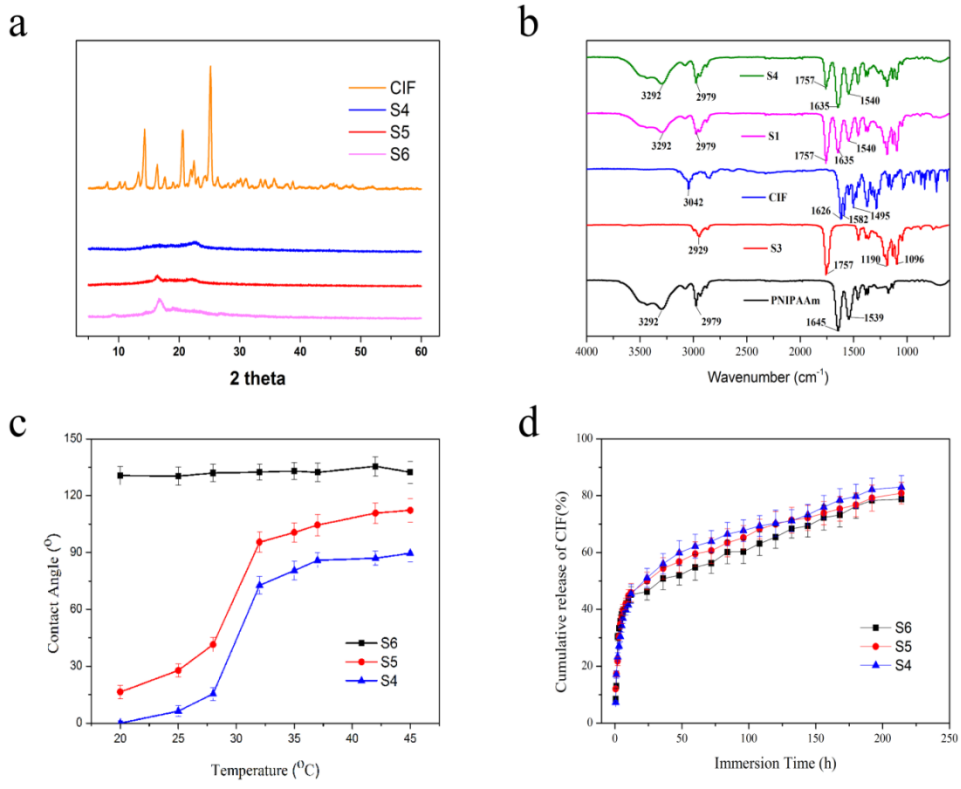

Fig. 2 a) XRD patterns of S4, S5, S6 and CIF; b) FTIR spectra of selected fibers, CIF and PNIPAAm; c) Water contact angles of S4, S5 and S6 as a function of temperature.; and, d) *In vitro* release profiles of CIF from S4, S5 and S6. For c) and d), data are reported as mean ± S.D. from three independent experiments

3.4 FTIR spectroscopy

Selected FITR spectra are presented in Fig. 2(b). PNIPAAm exhibits a broad band between around 3700 and 3100 cm^{-1}, which comprises a superposition of H-bonded N-H stretches (3296 cm^{-1}) and amide I and II combination and overtone bands [60]. Two characteristic peaks at 2979 cm^{-1} and 1635 cm^{-1} arise from C-H and C=O stretching vibrations, respectively. The distinct band at 1539 cm^{-1} results from C-N stretching and N-H bending vibrations. For the PLCL fibers (S3), two features at 2948 and 1757 cm^{-1} can be attributed to the stretching of $-CH_3$ and C=O groups, respectively. The stretching of the C-O-C moiety leads to other two peaks at 1183 and 1093 cm^{-1}[18]. The spectrum for CIF exhibits peaks at 3042 cm^{-1} (O-H stretching), 1626 cm^{-1} (C=O stretching), and numerous bands between 1582 and 1495 cm^{-1} from stretching vibrations of the benzene ring [47].

Considering the PLCL/PNIPAAm-based fibers S1 and S4, both have the distinct peaks of PNIPAAm (3292, 2979, 1635, 1540 cm^{-1}) and PLCL (1757 cm^{-1}). In S4, most of the characteristic peaks of CIF overlap with other vibrations from the polymers (which form the majority of the fiber mass). However, it can be seen that the peak at 1635 cm^{-1} is enhanced in S4 compared to the drug-free S1. This may be attributed to the presence of CIF. The FTIR spectra of the other fibers show similar features.

3.5 Thermosensitive behavior

The thermosensitive behavior of the fibers was explored in terms of contact angle, and the results are depicted in Fig. 2(c). The CA of S6 (PLCL/CIF fibers) remains at around 135° regardless of temperature. This agrees with previous studies [18], indicating the consistent hydrophobic nature of PLCL-based materials. The inclusion of thermosensitive PNIPAAm into S4 and S5 causes a distinct change in contact angle between 20 and 45 ºC. At 20 ºC, the CA of S5 is 16.4 ± 3.5° which rises to 112.3 ± 6.21° at 45 ºC. For S4, the CAs at 20 ºC and 45 ºC are approximately 0º and 89.7 ± 4.3°. The CAs of S4 are lower than those of S5 at each temperature. This is expected to result

from the greater proportion of hydrophobic PLCL in S5. The CAs increase dramatically at around 32°C, which is accordance with the reported LCST of PNIPAAm [29].

When the temperature is below the LCST, the C=O and N-H groups in the PNIPAAm chains will interact with water molecules to form intermolecular hydrogen bonds [61], which makes the fibers relatively hydrophilic below 32°C. When the temperature is increased to above the LCST, the PNIPAAm C=O and N-H groups tend to form intramolecular hydrogen bonds, leading to a collapsed globular conformation. As a result, water molecules find it difficult to interact with the C=O and N-H groups, resulting in hydrophobic fibers. It has been demonstrated that varying the temperature of PNIPAAm can effectively control cell adhesion and detachment [41]. Therefore, the thermosensitive properties of PNIPAAm can be exploited to reduce secondary injuries arising upon the replacement of wound dressings, and hence to accelerate healing. This idea has been verified in several reports [43-46, 62], and it therefore seems likely that PLCL/PNIPAAm thermosensitive fibers could also have promise in this regard.

3.6 Drug release

Fig. 2(d) shows the *in vitro* release behavior of CIF from the drug-loaded fibers (S4，S5 and S6). A similar burst release of around 45 % in the first *ca.* 15 hours can be seen from all three materials. This is thought to result from the presence of some CIF at or near the surface of the fibers; this can rapidly diffuse into the release milieu regardless of the solubility of the polymer constituents [59]. After this initial release, all three materials exhibit gradual release over 210 h. During the latter, the rate of CIF release is fastest from S4, followed by S5 and S6.

These different release behaviors can be explained by the fibers' surface wettability. The mechanism of drug release from polymers can involve diffusion, erosion, or a combination of both, and the release rate from a hydrophilic carrier tends to be faster than that from a hydrophobic material [59, 63]. The contact angle data (Section 3.5) demonstrate that S4, containing the highest proportion of PNIPAAm, has the highest wettability of the three systems at 37 ºC, followed by S5 and S6. This corresponds to the trend in the release rates (S4 > S5 > S6). At the end of the release

experiment, the cumulative release of CIF from S4, S5 and S6 reaches 83.1 ± 4.1 %, 80.9 ± 3.8 % and 78.8 ± 4.3 %, respectively. Thus, more than 15 % of the incorporated CIF was not released, with the release extent also correlating with wettability. The residual CIF is believed to be encapsulated deep inside the fibers.

These results of these *in vitro* release experiments demonstrate that PNIPAAm/PLCL composite fibers can sustain the release of CIF for more than 8 days. Although an *in vitro* experiment cannot be expected to mirror exactly what will happen *in vivo*, these results suggest that the fibers may be able to prevent wound infection for a number of days.

3.7 Antibacterial activity

Prior to exploring the the antibacterial properties of the fibers, the MICs of CIF were determined and found to be 12.5 μg/mL and 25 μg/mL against *E. coli* and *S. aureus*, respectively. As expected, CIF is high effective as an antibacterial agent.

The inhibition zone diameters of all the fiber samples are presented in Table 2, with representative images for S1 and S4 in Fig. 3. The inhibition zones of all the CIF-loaded fibers (S4, S5 and S6) are similar in size, indicating roughly constant antibacterial activities. On the contrary, there are no obvious inhibition zones with the drug-free samples (S1, S2 and S3). The potential of CIF in wound dressing materials has been demonstrated many times in the literature [64, 65], and the drug also has a low frequency of spontaneous resistance [66, 67]. In our previous work developing CIF-loaded PLLA / poly(di(ethylene glycol) methyl ether methacrylate) (PDEGMA) blend fibers we noted inhibition zones of 5.28 – 5.52 cm for *E. coli* and 5.21 – 5.52 cm for *S. aureus* after 24 h [47].The ability to avoid infection by exogenous organisms should accelerate the process of wound healing, and it appears that the systems produced here are similarly effective to those reported previously.

Table 2. Inhibition zone diameters for the fibers after 12 h of culture. Data are reported as mean ± S.D. from 6 independent experiments.

Sample	Inhibition zones against *E. coli* (cm)	Inhibition zones against *S. aureus* (cm)
S1	---	---
S2	---	---
S3	---	---
S4	5.21 ± 0.24	5.13 ± 0.20
S5	5.19 ± 0.11	5.17 ± 0.28
S6	5.24 ± 0.22	5.13 ± 0.16

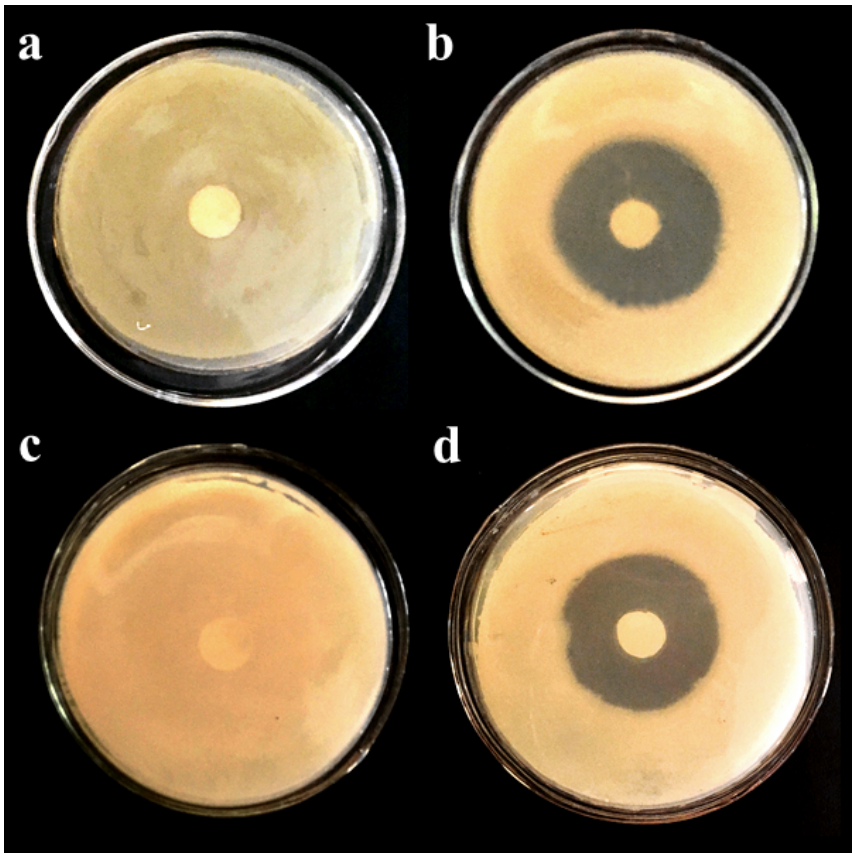

Fig. 3 Inhibition zones of selected fiber samples. Representative images of a) S1 against *E. coli*; b) S4 against *E.coli*; c) S1 against *S. aureus*; d) S4 against *S. aureus*, taken from 6 replicate experiments. The diameters of Petri dishes are 9.8 cm

3.8 Biocompatibility

According to the literature fibroblast cells play significant roles in wound healing, so L929 cells were used to explore the biocompatibility of the fibers [68]. In our previous work, we explored the cytotoxicity of a 0.9% CIF solution to L929 cells, and minimal cell death was identified [47]. This thus means that any cell death induced by the fibers is not a property of the incorporated antibiotic, but rather of the fibers themselves.

The results of MTT assays are depicted in Fig. 4. It is clear that the cells grew continuously from the 1st to the 5th day, both in the case of the untreated control and with all the fiber samples. The cell viabilities of cells exposed to the fibers are similar to those of the negative control group on day 1. After the 1st day, the S4 fibers (with the highest proportion of PNIPAAm) show the lowest cell viabilities. The viabilities are seen to be highest with the S6 fibers (PLCL alone, without PNIPAAm). The S6

viabilities were significantly greater than those of S4 on day 3 and 5 ($p < 0.05$). The numbers of cells cultured on S5 lay between these two extremes on days 3 and 5. These results indicate that L929 cells could proliferate on all the fiber samples (S4, S5 and S6), and thus all have good biocompatibility and are suitable as wound dressing materials. Moreover, the biocompatibility is enhanced by an increasing content of PLCL. This is expected to result from the greater cytocompatibility of PLCL than PNIPAAm; PLCL is widely known to be highly biocompatible [18, 69].

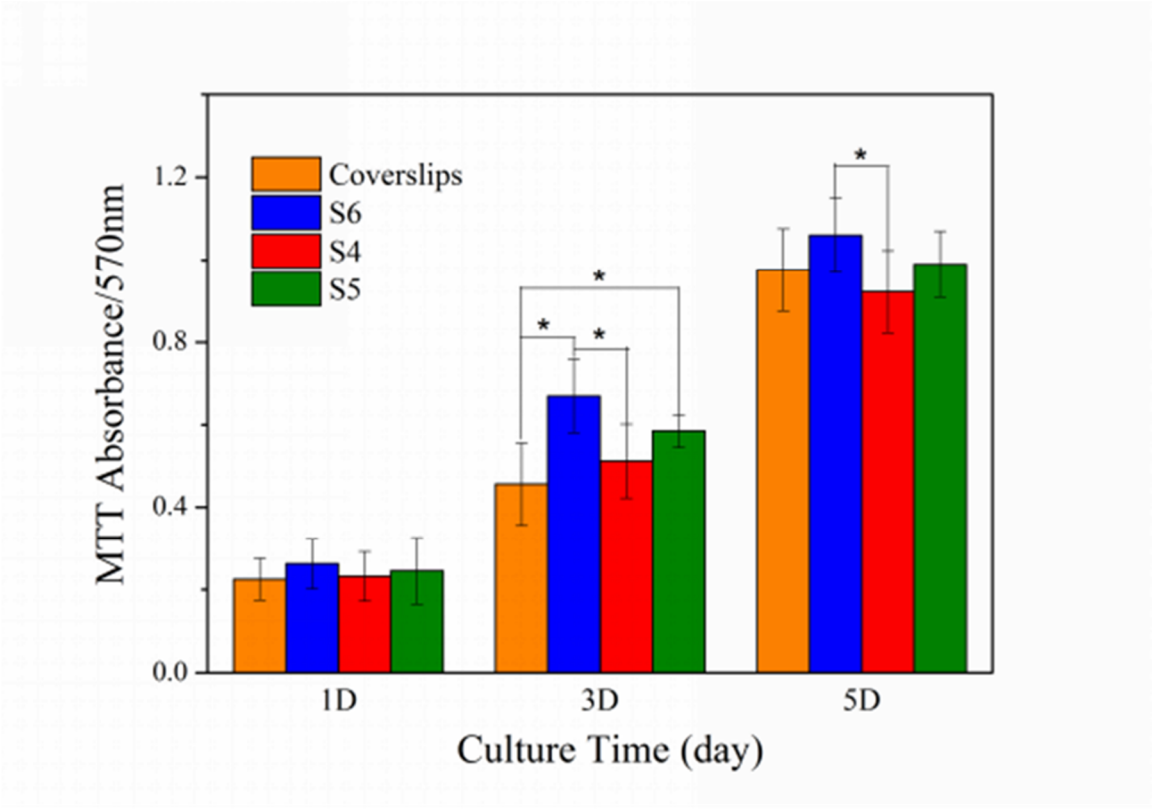

Fig. 4 Cell viability after exposure to the fibers for 1, 3, or 5 days. Data are given as mean ± S.D. from 3 independent experiments.

3.9 Macroscopic observations of wound healing

The macroscopic wound healing effects of S4, S5 and S6 were compared with a commercial gauze (Shanghai Yinjing Meidical Supplies Company Ltd.) immersed in a 0.9 % w/v CIF solution. Representative images of the wound healing process are given in Fig. 5. Around 3 h after the procedure, all the rats awoke and appeared healthy. The rats treated with the CIF-soaked gauze (Fig. 5(a)) displayed thicker scabs and larger

wound areas than those treated with the fibers (Fig. 5(b), (c) and (d)), indicating a slower healing rate. This can be explained considering the advantages that nanofibers offer as wound dressing materials. The size and topography of electrospun fiber mats can promote cell attachment and proliferation. Moreover, they allow gas and fluid uptake and exchange, and can hence absorb wound exudates. The prolonged period of drug release observed from these systems is also expected to contribute to the healing performance [1, 12, 50, 58, 70, 71].

Among the three fiber groups, the S4 and S5 mats were found to be easier to remove after treatment with cold saline, and they also have smaller wound areas than S6. At the end of the observation period (21 days), the scabs had largely healed and most of the wounds areas treated by S4 and S5 were filled with regenerated skin. The improved healing effects of S4 and S5 could be attributed to their thermosensitive properties (S6 has no such properties).

Fig. S3 illustrates the relative wound areas of the four groups from the 5^{th} to the 21^{st} day after operation. The results agree with the macroscopic observations in Fig. 5. After 5 days, the wound areas of all the samples were essentially the same. Subsequently, the different treatments lead to different rates of decline in the wound areas. After 21 days, S4 (6.50 ± 3.14 %) and S5 (7.71 ± 3.32 %) showed lower areas than S6 (14.36 ± 2.83 %) and the gauze group (24.81 ± 3.20 %). These results demonstrate that the CIF-loaded PNIPAAm/PLCL composite fibers could promote wound healing, performing better *in vivo* than a commercial gauze or the CIF-loaded PLCL fibers. The PNIPAAm/PLCL materials are approximately equally effective with the PDEGMA/PLCL systems reported previously [47]. The best performing PDEGMA/PLCL fiber formulation reduced the wound area to 5.7 ± 0.8 % of the original area, which is very close to the values determined for S4 and S6 here. Therefore, it appears that PNIPAAm can recapitulate the effects of PDEGMA in these wound dressings, suggesting that a wide range of thermoresponsive polymers can be employed in the development of clinical wound dressing products.

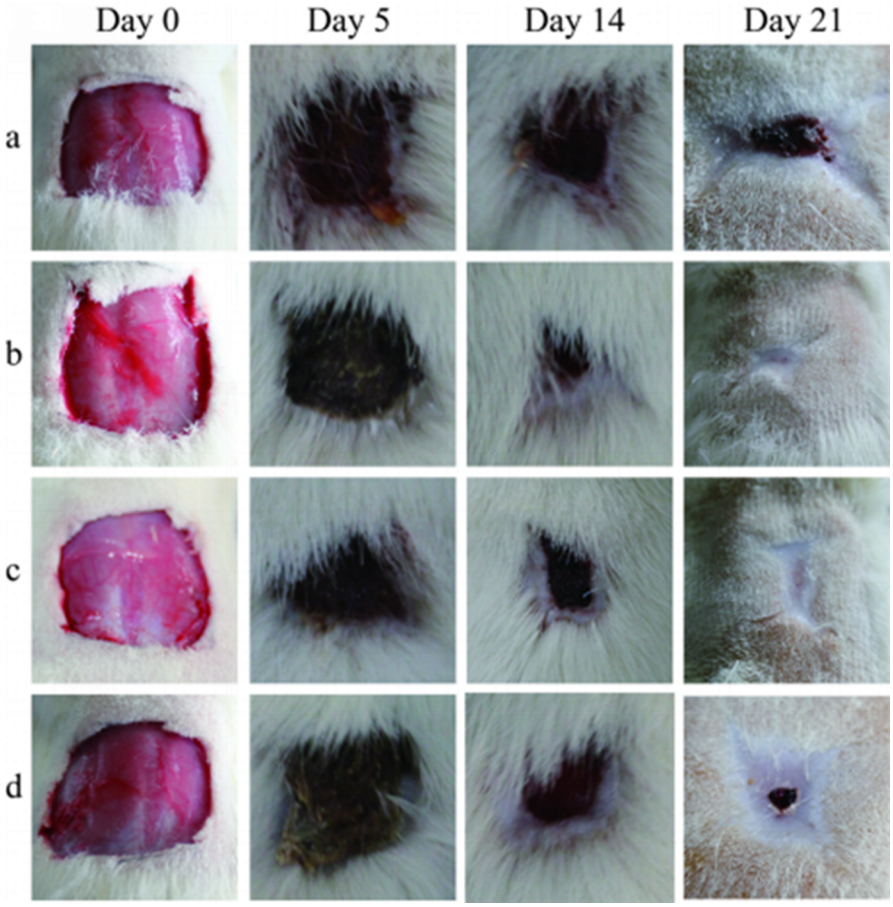

Fig. 5 Representative images of skin wounds treated with selected samples for 0, 5, 14 and 21 days post-operation. The wounds were treated with (a) a commercial gauze soaked with 0.9% CIF solution, (b) S4, (c) S5 and (d) S6.

3.10 Histological examinations

HE staining images of the tissues treated by S4, S5, S6 and gauze are displayed in Fig. 6, together with a section of healthy skin without any wound or treatment. Regenerated epidermis can be seen at the edge of the wounds in all groups, and is marked with circles in Fig. 6. With the group treated by the CIF-soaked gauze (Fig. 6(a)), the epidermis is thinner and more irregular than that with the groups treated using fiber dressings (Fig. 6(b)-(d)). The epidermis of the S6 group (Fig. 6(d)) is more regular than that of the gauze group, but the wounds covered by S4 (Fig. 6(b)) and S5 (Fig. 6(c)) showed the best healing results. The continuity and regularity of the epidermis in these two groups is the closet to normal skin (Fig. 6(e)). Moreover, the basal cells of rats treated with S4 and S5 (marked by white arrows) exhibit more uniform shapes and more regular

arrangements than other treatment groups. These results accord with the macroscopic observations of the wound healing (Section 3.9), and further demonstrate the improved healing effects of PNIPAAm/PLCL fibers loaded with CIF over other groups.

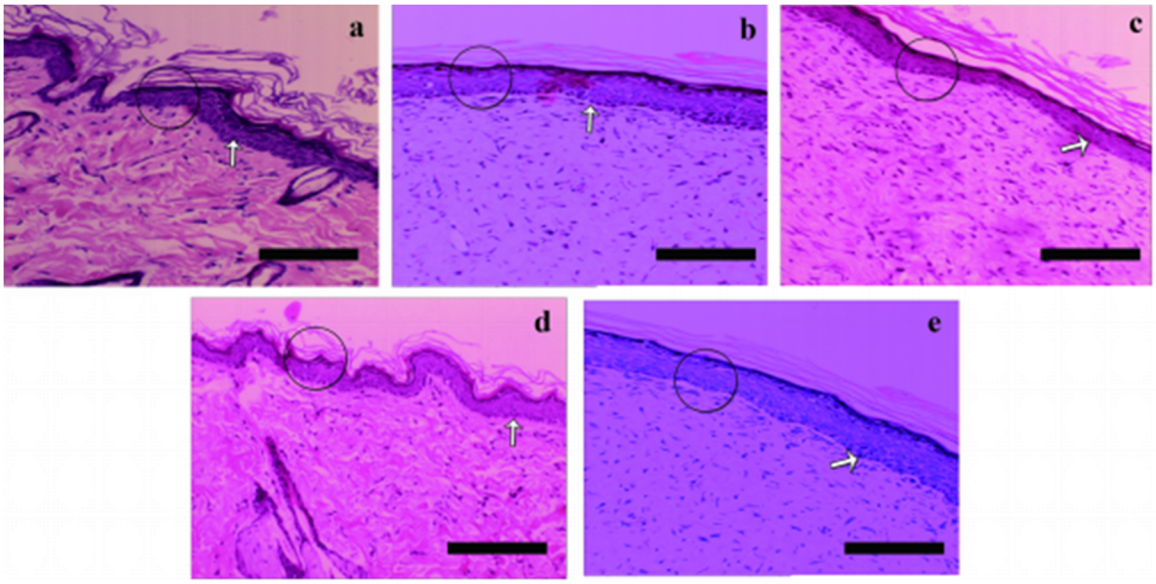

Fig. 6 HE staining for the epithelialization of skin wounds treated for 21 days with (a) a commercial gauze soaked with 0.9% CIF solution, (b) S4, (c) S5, (d) S6 and (e) healthy skin where no wound has been inflicted. Scale bars represent 200 μm.

4. Conclusions

In this study, thermosensitive poly(N-isopropylacrylamide) (PNIPAAm) was blended with (poly(l-lactic acid-co-ε-caprolactone)) (PLCL) and processed into fibers by electrospinning. The antibiotic ciprofloxacin (CIF) was also incorporated into the composite fibers. The fibers show generally smooth and cylindrical morphologies, and the addition of CIF was found to reduce the diameters of the fibers compared to analogous systems made with the polymer blend alone. XRD analysis indicated that CIF was dispersed in the fibers in an amorphous state. The water contact angle of the fiber mats is highly dependent on the temperature, with the wettability of the PNIPAAm/PLCL fibers declining abruptly at around 32 ºC. *In vitro* drug release experiments demonstrate that CIF could be gradually released from the fibers over 200 h. The CIF-loaded composite fibers show good antibacterial activity against *E. coli* and

S. Aureus. They also exhibit promising biocompatibility and can promote the proliferation of L929 fibroblasts. *In vivo* wound healing observations and histological examinations showed that PNIPAAm/PLCL fibers loaded with CIF were able to accelerate healing, and the blend fibers perform better than those containing only PLCL and CIF. These results thus demonstrate the potential of PNIPAAm/PLCL fibers loaded with CIF as potent wound dressing materials.

Acknowledgements

This investigation was supported by grant 16410723700 from the Science and Technology Commission of Shanghai Municipality, the Biomedical Textile Materials "111 Project" of the Ministry of Education of China (No. B07024), and the UK-China Joint Laboratory for Therapeutic Textiles (based at Donghua University).

References

[1] Zahedi, P., Rezaeian, I., Ranaei-Siadat, S. O., Jafari, S. H., & Supaphol, P. (2010). A review on wound dressings with an emphasis on electrospun nanofibrous polymeric bandages. *Polymers for Advanced Technologies*, *21*, 77-95.

[2] Seaman, S. (2002). Dressing selection in chronic wound management. *Journal of the American Podiatric Medical Association*, *92*, 24-33.

[3] Dongargaonkar, A. A., Bowlin, G. L., & Yang, H. (2013). Electrospun blends of gelatin and gelatin-dendrimer conjugates as a wound-dressing and drug-delivery platform. *Biomacromolecules, 14*, 4038-4045.

[4] Boateng, J. S., Matthews, K. H., Stevens, H. N., & Eccleston, G. M. (2008). Wound healing dressings and drug delivery systems: a review. *Journal of Pharmaceutical Sciences*, *97*(8), 2892-2923.

[5] Cho, Y. S., Lee, J. W., Lee, J. S., Lee, J. H., Yoon, T. R., Kuroyanagi, Y., Park, M. H., & Kim, H. J. (2002). Hyaluronic acid and silver sulfadiazine-impregnated polyurethane foams for wound dressing application. *Journal of Materials Science: Materials in Medicine*, *13*(9), 861-865.

[6] Mi, L., Xue, H., Li, Y., & Jiang, S. (2011). A thermoresponsive antimicrobial wound

dressing hydrogel based on a cationic betaine ester. *Advanced Functional Materials*, *21*(21), 4028-4034.

[7] Gonzalez, J. S., Ludueña, L. N., Ponce, A., & Alvarez, V. A. (2014). Poly (vinyl alcohol)/cellulose nanowhiskers nanocomposite hydrogels for potential wound dressings. *Materials Science and Engineering: C*, *34*, 54-61..

[8] Newman, G. R., Walker, M., Hobot, J. A., & Bowler, P. G. (2006). Visualisation of bacterial sequestration and bactericidal activity within hydrating Hydrofiber® wound dressings. *Biomaterials*, *27*(7), 1129-1139.

[9] Lannutti, J., Reneker, D., Ma, T., Tomasko, D., & Farson, D. (2007). Electrospinning for tissue engineering scaffolds. *Materials Science and Engineering: C*, *27*(3), 504-509.

[10] Meng, Z. X., Wang, Y. S., Ma, C., Zheng, W., Li, L., & Zheng, Y. F. (2010). Electrospinning of PLGA/gelatin randomly-oriented and aligned nanofibers as potential scaffold in tissue engineering. *Materials Science and Engineering: C*, *30*(8), 1204-1210.

[11] Gautam, S., Dinda, A. K., & Mishra, N. C. (2013). Fabrication and characterization of PCL/gelatin composite nanofibrous scaffold for tissue engineering applications by electrospinning method. *Materials Science and Engineering: C*, *33*(3), 1228-1235.

[12] Zhang, Y., Lim, C. T., Ramakrishna, S., & Huang, Z. M. (2005). Recent development of polymer nanofibers for biomedical and biotechnological applications. *Journal of Materials Science: Materials in Medicine*, *16*, 933-946.

[13] Venugopal, J., & Ramakrishna, S. (2005). Applications of polymer nanofibers in biomedicine and biotechnology. *Applied Biochemistry and Biotechnology*, *125*, 147-157.

[14] Gu, S. Y., Wang, Z. M., Ren, J., & Zhang, C. Y. (2009). Electrospinning of gelatin and gelatin/poly (l-lactide) blend and its characteristics for wound dressing. *Materials Science and Engineering: C*, *29*(6), 1822-1828.

[15] Lee, C. H., Chang, S. H., Chen, W. J., Hung, K. C., Lin, Y. H., Liu, S. J., ... & Juang, J. H. (2015). Augmentation of diabetic wound healing and enhancement of collagen content using nanofibrous glucophage-loaded collagen/PLGA scaffold

membranes. *Journal of Colloid and Interface Science*, *439*, 88-97.

[16] Ranjbar-Mohammadi, M., Bahrami, S. H., & Joghataei, M. T. (2013). Fabrication of novel nanofiber scaffolds from gum tragacanth/poly (vinyl alcohol) for wound dressing application: in vitro evaluation and antibacterial properties. *Materials Science and Engineering: C*, *33*(8), 4935-4943.

[17] Li, H., Wu, T., Zheng, Y., El-Hamshary, H., Al-Deyab, S. S., & Mo, X. (2014). Fabrication and characterization of Mg/P (LLA-CL)-blended nanofiber scaffold. *Journal of Biomaterials Science, Polymer Edition*, *25*, 1013-1027.

[18] Wu, T., Jiang, B., Wang, Y., Yin, A., Huang, C., Wang, S., & Mo, X. (2015). Electrospun poly (l-lactide-co-caprolactone)–collagen–chitosan vascular graft in a canine femoral artery model. *Journal of Materials Chemistry B*, *3*, 5760-5768.

[19] Lee, J., Tae, G., Kim, Y. H., Park, I. S., Kim, S. H., & Kim, S. H. (2008). The effect of gelatin incorporation into electrospun poly (l-lactide-co-ε-caprolactone) fibers on mechanical properties and cytocompatibility. *Biomaterials*, *29*(12), 1872-1879.

[20] Qiu, S., Liu, L., Wang, B., Shen, F., Zhang, W., Li, M., & Ma, Y. (2005). Facile synthesis of carbazole-containing semiladder polyphenylenes for pure-blue electroluminescence. *Macromolecules*, *38*(16), 6782-6788.

[21] Ying, L., Kang, E. T., Neoh, K. G., Kato, K., & Iwata, H. (2004). Drug permeation through temperature-sensitive membranes prepared from poly (vinylidene fluoride) with grafted poly (N-isopropylacrylamide) chains. *Journal of Membrane Science*, *243*(1), 253-262.

[22] Lacerda, L., Parize, A. L., Fávere, V., Laranjeira, M. C. M., & Stulzer, H. K. (2014). Development and evaluation of pH-sensitive sodium alginate/chitosan microparticles containing the antituberculosis drug rifampicin. *Materials Science and Engineering: C*, *39*, 161-167.

[23] Lin, C., Zhao, P., Li, F., Guo, F., Li, Z., & Wen, X. (2010). Thermosensitive in situ-forming dextran–pluronic hydrogels through Michael addition. *Materials Science and Engineering: C*, *30*(8), 1236-1244.

[24] Xu, F. J., Kang, E. T., & Neoh, K. G. (2006). pH-and temperature-responsive hydrogels from crosslinked triblock copolymers prepared via consecutive atom transfer

radical polymerizations. *Biomaterials*, *27*(14), 2787-2797.

[25] Zhang, X. Z., Lewis, P. J., & Chu, C. C. (2005). Fabrication and characterization of a smart drug delivery system: microsphere in hydrogel. *Biomaterials*, *26*(16), 3299-3309.

[26] Chen, S., Zhong, H., Gu, B., Wang, Y., Li, X., Cheng, Z., ... & Yao, C. (2012). Thermosensitive phase behavior and drug release of in situ N-isopropylacrylamide copolymer. *Materials Science and Engineering: C*, *32*(8), 2199-2204.

[27] Wenceslau, A. C., dos Santos, F. G., Ramos, É. R., Nakamura, C. V., Rubira, A. F., & Muniz, E. C. (2012). Thermo-and pH-sensitive IPN hydrogels based on PNIPAAm and PVA-Ma networks with LCST tailored close to human body temperature. *Materials Science and Engineering: C*, *32*(5), 1259-1265.

[28] Schmaljohann, D. (2006). Thermo-and pH-responsive polymers in drug delivery. *Advanced drug delivery reviews*, *58*(15), 1655-1670.

[29] Plunkett, K. N., Zhu, X., Moore, J. S., & Leckband, D. E. (2006). PNIPAM chain collapse depends on the molecular weight and grafting density. *Langmuir*, *22*(9), 4259-4266.

[30] Mayo−Pedrosa, M., Alvarez−Lorenzo, C., Lacík, I., Martinez−Pacheco, R., & Concheiro, A. (2007). Sustained release pellets based on poly (N−isopropyl acrylamide): Matrix and in situ photopolymerization−coated systems. *Journal of Pharmaceutical Sciences*, *96*(1), 93-105.

[31] Yim, H., Kent, M. S., Mendez, S., Balamurugan, S. S., Balamurugan, S., Lopez, G. P., & Satija, S. (2004). Temperature-dependent conformational change of PNIPAM grafted chains at high surface density in water. *Macromolecules*, *37*(5), 1994-1997.

[32] Huang, S. R., Lin, K. F., Lee, C. F., & Chiu, W. Y. (2014). Synthesis and properties of thermoresponsive magnetic polymer composites and their electrospun nanofibers. *Journal of Polymer Science Part A: Polymer Chemistry*, *52*(6), 848-856.

[33] Rockwood, D. N., Chase, D. B., Akins, R. E., & Rabolt, J. F. (2008). Characterization of electrospun poly (N-isopropyl acrylamide) fibers. *Polymer*, *49*(18), 4025-4032.

[34] Kumoda, M., Takeoka, Y., & Watanabe, M. (2003). Template synthesis of poly (N-

isopropylacrylamide) minigels using interconnecting macroporous polystyrene. *Langmuir*, *19*(3), 525-528.

[35] Song, M., Pan, C., Li, J., Zhang, R., Wang, X., & Gu, Z. (2008). Blends of TiO 2 nanoparticles and poly (N-isopropylacrylamide)-co-polystyrene nanofibers as a means to promote the biorecognition of an anticancer drug. *Talanta*, *75*(4), 1035-1040.

[36] Yamato, M., Akiyama, Y., Kobayashi, J., Yang, J., Kikuchi, A., & Okano, T. (2007). Temperature-responsive cell culture surfaces for regenerative medicine with cell sheet engineering. *Progress in Polymer Science*, *32*(8), 1123-1133.

[37] París, R., & Quijada‐Garrido, I. (2009). Swelling and hydrolytic degradation behaviour of pH‐responsive hydrogels of poly [(N‐isopropylacrylamide)‐co‐(methacrylic acid)] crosslinked by biodegradable polycaprolactone chains. *Polymer International*, *58*(4), 362-367.

[38] Lee, W. F., & Cheng, T. S. (2008). Studies on preparation and properties of porous biodegradable poly (NIPAAm) hydrogels. *Journal of Applied Polymer Science*, *109*(3), 1982-1992.

[39] Lin, X., Tang, D., Cui, W., & Cheng, Y. (2012). Controllable drug release of electrospun thermoresponsive poly(n-isopropylacrylamide)/poly(2-acrylamido-2-methylpropanesulfonic acid) nanofibers. *Journal of Biomedical Materials Research Part A*, 100(7), 1839-45.

[40] Wang, N., Zhao, Y., & Jiang, L. (2008). Low-cost, thermoresponsive wettability of surfaces: poly(n-isopropylacrylamide)/polystyrene composite films prepared by electrospinning. *Macromolecular Rapid Communications*, 29(29), 485-489.

[41] Schild, H. G. (1992). Poly (N-isopropylacrylamide): experiment, theory and application. *Progress in Polymer Science*, *17*(2), 163-249.

[42] Akiyama, Y., Kikuchi, A., Yamato, M., & Okano, T. (2004). Ultrathin poly (N-isopropylacrylamide) grafted layer on polystyrene surfaces for cell adhesion/detachment control. *Langmuir*, *20*(13), 5506-5511.

[43] Wang, L. S., Chow, P. Y., Phan, T. T., Lim, I. J., & Yang, Y. Y. (2006). Fabrication and characterization of nanostructured and thermosensitive polymer membranes for wound healing and cell grafting. *Advanced Functional Materials*, *16*(9), 1171-1178.

[44] Heilmann, S., Küchler, S., Wischke, C., Lendlein, A., Stein, C., & Schäfer-Korting, M. (2013). A thermosensitive morphine-containing hydrogel for the treatment of large-scale skin wounds. *International Journal of Pharmaceutics*, *444*(1), 96-102.

[45] Reddy, T. T., Kano, A., Maruyama, A., Hadano, M., & Takahara, A. (2008). Thermosensitive transparent semi-interpenetrating polymer networks for wound dressing and cell adhesion control. *Biomacromolecules*, *9*(4), 1313-1321.

[46] Yang, J. M., Shu, J. Y., Hao, T. L., Wu, T. H., & Chen, H. J. (2008). Chitosan containing PU/poly(NIPAAm) thermosensitive membrane for wound dressing. *Materials Science & Engineering C*, 28(1), 150-156.

[47] Li, H., Williams, G. R., Wu, J., Lv, Y., Sun, X., Wu, H., Zhu, L. M. (2016). Thermosensitive nanofibers loaded with ciprofloxacin as antibacterial wound dressing materials. *International Journal of Pharmaceutics*, *517*(1),135-147.

[48] Hu, J., Li, H. Y., Williams, G. R., Yang, H. H., Tao, L., & Zhu, L. M. (2016). Electrospun Poly (N-isopropylacrylamide)/ethyl cellulose nanofibers as thermoresponsive drug delivery systems. *Journal of Pharmaceutical Sciences*, 105(3), 1104-1112

[49] Unnithan, A. R., Barakat, N. A., Pichiah, P. T., Gnanasekaran, G., Nirmala, R., Cha, Y. S., Jung, C. H. El-Newehy, M., & Kim, H. Y. (2012). Wound-dressing materials with antibacterial activity from electrospun polyurethane–dextran nanofiber mats containing ciprofloxacin HCl. *Carbohydrate Polymers*, *90*(4), 1786-1793.

[50] Jin, M., Yu, D. G., Wang, X., Geraldes, C. F., Williams, G. R., Bligh, S. W. (2016). Electrospun contrast agent loaded fibers for colon‐targeted MRI. *Advanced Healthcare Materials*, *5*(8), 977-985.

[51] Andrews, J. M. (2001). Determination of minimum inhibitory concentrations. *Journal of Antimicrobial Chemotherapy*, *48* (suppl 1), 5-16.

[52] Yang, Y., Xia, T., Zhi, W., Wei, L., Weng, J., Zhang, C., & Li, X. (2011). Promotion of skin regeneration in diabetic rats by electrospun core-sheath fibers loaded with basic fibroblast growth factor. *Biomaterials*, *32*(18), 4243-4254.

[53] Tokuhiro, T., Amiya, T., Mamada, A., & Tanaka, T. (1991). NMR study of poly (N-isopropylacrylamide) gels near phase transition. *Macromolecules*, *24*(10), 2936-

2943.

[54] Pham, Q. P., Sharma, U., & Mikos, A. G. (2006). Electrospinning of polymeric nanofibers for tissue engineering applications: a review. *Tissue Engineering*, *12*(5), 1197-1211.

[55] Sheng, X., Fan, L., He, C., Zhang, K., Mo, X., Wang, H. (2013). Vitamin E-loaded silk fibroin nanofibrous mats fabricated by green process for skin care application. *International Journal of Biological Macromolecules*, *56*, 49-56.

[56] Yan, S., Xiaoqiang, L., Shuiping, L., Xiumei, M., & Ramakrishna, S. (2009). Controlled release of dual drugs from emulsion electrospun nanofibrous mats. *Colloids and Surfaces B: Biointerfaces*, *73*(2), 376-381.

[57] Yang, C., Yu, D. G., Pan, D., Liu, X. K., Wang, X., Bligh, S. A., Williams, G. R. (2016). Electrospun pH-sensitive core–shell polymer nanocomposites fabricated using a tri-axial process. *Acta Biomaterialia*, *35*, 77-86.

[58] Jia, Y. T., Gong, J., Gu, X. H., Kim, H. Y., Dong, J.,Shen, X. Y. (2007). Fabrication and characterization of poly (vinyl alcohol)/chitosan blend nanofibers produced by electrospinning method. *Carbohydrate Polymers*, *67*(3), 403-409.

[59] Li, H., Wang, M., Williams, G. R., Wu, J., Sun, X., Lv, Y., Zhu, L. M. (2016). Electrospun gelatin nanofibers loaded with vitamins A and E as antibacterial wound dressing materials. *RSC Advances*, *6*(55), 50267-50277.

[60] Lizundia, E., Meaurio, E., Laza, J. M., Vilas, J. L., & Isidro, L. L. (2015). Study of the chain microstructure effects on the resulting thermal properties of poly (L-lactide)/poly (N-isopropylacrylamide) biomedical materials. *Materials Science and Engineering: C*, *50*, 97-106.

[61] Lin, X., Tang, D., Gu, S., Du, H., & Jiang, E. (2013). Electrospun poly (N-isopropylacrylamide)/poly (caprolactone)-based polyurethane nanofibers as drug carriers and temperature-controlled release. *New Journal of Chemistry*, *37*(8), 2433-2439.

[62] Rezapour-Lactoee, A., Yeganeh, H., Ostad, S. N., Gharibi, R., Mazaheri, Z., Ai, J. (2016). Thermoresponsive polyurethane/siloxane membrane for wound dressing and cell sheet transplantation: In-vitro and in-vivo studies. *Materials Science and*

Engineering: C, *69*, 804-814.

[63] Dong, Y., Zhang, Z., Feng, S. S. (2008). d-α-Tocopheryl polyethylene glycol 1000 succinate (TPGS) modified poly (l-lactide)(PLLA) films for localized delivery of paclitaxel. *International Journal of Pharmaceutics*, *350*(1), 166-171.

[64] Unnithan, A. R., Barakat, N. A., Pichiah, P. T., Gnanasekaran, G., Nirmala, R., Cha, Y. S., Jung, C.H., El-Newehy, M., Kim, H. Y. (2012). Wound-dressing materials with antibacterial activity from electrospun polyurethane–dextran nanofiber mats containing ciprofloxacin HCl. *Carbohydrate Polymers*, *90*(4), 1786-1793.

[65] Tsou, T. L., Tang, S. T., Huang, Y. C., Wu, J. R., Young, J. J., Wang, H. J. (2005). Poly (2-hydroxyethyl methacrylate) wound dressing containing ciprofloxacin and its drug release studies. *Journal of Materials Science: Materials in Medicine*, *16*(2), 95-100.

[66] Yu, H., Xu, X., Chen, X., Hao, J., Jing, X. (2006). Medicated wound dressings based on poly (vinyl alcohol)/poly (N−vinyl pyrrolidone)/chitosan hydrogels. *Journal of Applied Polymer Science*, *101*(4), 2453-2463.

[67] Dillen, K., Vandervoort, J., Van den Mooter, G., Verheyden, L., Ludwig, A. (2004). Factorial design, physicochemical characterisation and activity of ciprofloxacin-PLGA nanoparticles. *International Journal of Pharmaceutics*, *275*(1), 171-187.

[68] Cook, H., Stephens, P., Davies, K. J., Harding, K. G., & Thomas, D. W. (2000). Defective extracellular matrix reorganization by chronic wound fibroblasts is associated with alterations in TIMP-1, TIMP-2, and MMP-2 activity. *Journal of Investigative Dermatology*, *115*(2), 225-233.

[69] Wu, T., Zheng, H., Chen, J., Wang, Y., Sun, B., Morsi, Y., El-Hamshary, H., Al-Deyab, S.S., Chen, C., Mo, X. (2017). Application of a bilayer tubular scaffold based on electrospun poly (l-lactide-co-caprolactone)/collagen fibers and yarns for tracheal tissue engineering. *Journal of Materials Chemistry B*, *5*(1), 139-150.

[70] Rath, G., Hussain, T., Chauhan, G., Garg, T., Goyal, A. K. (2016). Development and characterization of cefazolin loaded zinc oxide nanoparticles composite gelatin nanofiber mats for postoperative surgical wounds. *Materials Science and Engineering: C*, *58*, 242-253.

[71] Zou, B., Li, X., Zhuang, H., Cui, W., Zou, J., & Chen, J. (2011). Degradation behaviors of electrospun fibrous composites of hydroxyapatite and chemically modified poly (DL-lactide). *Polymer Degradation and Stability*, *96*(1), 114-122.